

**Nanostructured interfaces for probing and facilitating extracellular electron transfer**

Journal:	<i>Journal of Materials Chemistry B</i>
Manuscript ID	TB-REV-06-2018-001598.R1
Article Type:	Review Article
Date Submitted by the Author:	08-Jul-2018
Complete List of Authors:	Hsu, Leo (Huan-Hsuan); Tufts University, Department of Biomedical Engineering Deng, Pu; Tufts University, Department of Biomedical Engineering Zhang, Yixin; Tufts University, Department of Biomedical Engineering Nguyen, Han; Tufts University, Department of Biomedical Engineering Jiang, Xiaocheng; Tufts University, Department of Biomedical Engineering



Journal Name

ARTICLE

## Nanostructured interfaces for probing and facilitating extracellular electron transfer

Leo (Huan-Hsuan) Hsu, Pu Deng, Yixin Zhang, Han N. Nguyen and Xiaocheng Jiang\*

Received 00th January 20xx,  
Accepted 00th January 20xx

DOI: 10.1039/x0xx00000x

www.rsc.org/

Extracellular electron transfer (EET) is a process performed by electrochemically active bacteria (EAB) to transport metabolically-generated electrons to external solid-phase acceptors through specific molecular pathways. Naturally bridging biotic and abiotic charge transport systems, EET offers ample opportunities in a wide range of bio-interfacing applications, from renewable energy conversion, resource recovery, to bioelectronics. Full exploration of EET fundamentals and implications demands technologies that could seamlessly interface and interrogate with key components and processes at relevant length scales. In this review, we will discuss the recent development of nanoscale platforms that enabled EET investigation from single-cell to network levels. We will further overview research strategies in utilizing rationally designed and integrated nanomaterials for EET facilitation and efficiency enhancements. In the future, EET components such as C-cytochrome based outer membranes and bacterial nanowires along with their assembled structures present themselves as a whole new category of biosynthetic electroactive materials with genetically encoded functionality and intrinsic biocompatibility, opening up possibilities to revolutionize the way electronic devices communicate with biological systems.

### 1 I. Introduction

2 All essential life-sustaining biological processes, such as  
3 photosynthesis and cellular respiration, are achieved through a  
4 cascade of electron transfers.<sup>1</sup> In most cases, this enzyme-driven  
5 process is accomplished intracellularly through a series of  
6 biochemical reactions at molecular length scales. Interestingly  
7 certain microorganisms – usually referred as electrochemically  
8 active bacteria (EAB) - are able to set-up long-range (>100 μm) and  
9 long-term stable (years) electrical connections with extracellular  
10 electron acceptors.<sup>2</sup> This extracellular electron transfer (EET)  
11 process usually occurs under soluble electron acceptor limited  
12 conditions, where EABs can perform as catalysts to directly transfer  
13 their respiratory electrons across outer membranes to external  
14 solid-state electron acceptors. EET stands out as a unique model  
15 system as it breaks the biotic-abiotic boundary to achieve direct  
16 energy conversion from biochemical to electrical forms, thus  
17 demonstrating potentials in various applications, including energy  
18 harvesting,<sup>3</sup> resource recovery,<sup>4</sup> and materials synthesis.  
19 Moreover, deeper understanding of EET can reveal the fundamental  
20 of biological electron transfer processes, which are extremely  
21 valuable for both life sciences studies as well as technological  
22 advancements in interdisciplinary research fields, such as the brain

23 machine interface<sup>6,7</sup> that require communication between  
24 biological systems and electronic components. However, the  
25 underlying principles of EET are still vague and under active debate  
26 due to limitations posed by conventional strategies in interfacing  
27 and interrogating EET at relevant length scales. To tackle these  
28 challenges, current advances in nanotechnology have opened up  
29 opportunities that allow researchers to rationally control and  
30 modulate EET pathways to unambiguously determine the key  
31 mechanisms and limits and ultimately improve EET efficiency.<sup>8</sup> In  
32 this review, firstly, we will discuss the state-of-the-art studies of  
33 EET's mechanisms, its implications, and several obstacles faced by  
34 researchers in the fields. Secondly, contributions of nanotechnology  
35 to EET investigations are introduced in which EET can be precisely  
36 probed down to single-bacterium level, thus identifying the key  
37 limiting factors in current applications. Lastly, we summarize recent  
38 progress in the design and integration of functional nanomaterials  
39 to facilitate EET, which holds the potential to inspire novel  
40 approaches to further optimize the coupling of biotic EET pathway  
41 with abiotic electrodes and broaden various EET's applications.

### II. EET: Mechanisms and Implications

#### A. EET Mechanisms

42 In the last decades, much effort has been put into investigating EET  
43 mechanisms, which have been shown to occur via both indirect and  
44 direct routes.<sup>2</sup> In the indirect EET process, EABs secrete small redox-  
45 active molecules, such as phenazines,<sup>9</sup> flavins,<sup>10</sup> and quinones,<sup>11</sup> to  
46 facilitate the transfer of metabolically-generated electrons to  
47 extracellular acceptors. In ideal conditions, these molecules can re-  
48 enter the bacteria's bodies and repeatedly aid the electron transfer  
49 process.

\* Department of Biomedical Engineering, Tufts University, Medford, Massachusetts  
02155, USA. E-mail: Xiaocheng.Jiang@tufts.edu

† Footnotes relating to the title and/or authors should appear here.  
Electronic Supplementary Information (ESI) available: [details of any  
supplementary information available should be included here].  
DOI: 10.1039/x0xx00000x

1 process; hence, they are commonly referred to as “electron shuttles.” Besides indirect EET, EABs are also capable of directly transferring electrons through their outer membranes by electron tunnelling or performing redox reactions with closely-contacted extracellular electron acceptors. It has been identified that this direct EET process is mainly accomplished through a cascade of electron transfer processes carried out by a series of surface redox proteins – C type cytochromes (cyts).<sup>12–14</sup> In cases where they need to make contact with further-away electron acceptors, EABs can form various micro- to nano-scale extracellular structures to facilitate long-range EET processes. Recent research demonstrated that two most common EAB species: *Shewanella* and *Geobacter*, can develop pilus-like structures – usually referred to as bacterial nanowire (BNWs) – to remotely access extracellular electron acceptors.<sup>15–17</sup> Two different EET models have been proposed to elucidate the electron transfer mechanism in BNWs, namely: (i) metallic-like electron transfer and (ii) electron hopping. In metallic-like electron transfer model, electrons are hypothesized to transfer through overlapping  $\pi$ - $\pi$  orbitals of aromatic amino acids in BNWs, which shares similar mechanisms to synthetic organic conducting polymers.<sup>18</sup> On the other hand, in electron hopping model, electron transfer is completed by a series of redox reactions through closely aligned cyts along BNW, which can be illustrated by the well-understood electron hopping mechanism of redox polymers.<sup>19–22</sup>

26 Moreover, in order to gain deeper understanding of each individual cyt’s function, genetic engineering is performed, allowing for the expression or deletion of certain cyts in biofilm.<sup>12,14,23–27</sup> The EET efficiencies of these mutant biofilms can be evaluated by current generation through a microbial fuel cell setup (introduced in next section) or metal oxide reduction experiments. Besides, cyclic voltammeteries are commonly applied to study the EET dynamics of both wild-type EABs and their mutants,<sup>14,28</sup> from which the functions of individual cyt in EET can be precisely identified. These works are systematically covered in several reviews.<sup>25,26</sup> To summarize, in *Geobacter*, metabolically-generated electrons are transferred from the cytoplasm to outer membrane by periplasmic cyts (e.g. PpcA). Then, outer membrane c-type cytochrome EET processes are mainly facilitated by outer membrane c-type cytochrome (OmcZ) and *Geobacter* BNWs (also known as Type-IV pili). These EET processes are also supported by other OMCs (e.g. OmcB, OmcE, and OmcS).<sup>14</sup> In *Shewanella*, the cross-membrane electron transport is carried out by CymA (tetrahaem cytochrome c), followed by transfer to external electron acceptors through metal reduction proteins (e.g. MtrA, MtrB and MtrC).<sup>23,25</sup> Self-excreted flavins play a role in this EET process as electron shuttles.<sup>10</sup> Alternatively, *Shewanella* BNWs are shown to be extensions of the bacterial outer membrane which allow electrons to hop to remote electron acceptors via the membrane-bound MtrABC–OmcA tetramers.<sup>16</sup>

50 Electrochemical impedance spectroscopy (EIS) is another useful tool to quantitatively investigate EET, which is capable of differentiating the charge transfer resistances of biofilm and the contact resistances between biofilms and electrodes.<sup>29</sup> These studies show that the electrical contact at biofilm/electrode interface can be effectively improved by replacing the metal electrode with carbon-based materials as well as increasing electrode surface area. Duff

biofilm development, the charge transfer resistances naturally decrease as a result of the involvement of additional EET pathways.

## B. EET Implications

Capable of catalysing both electrical and chemical energy conversions, EET piques growing interest in its implications. Energy harvesting is the most well-developed application of EET, which can be achieved by incorporating EABs in the anode of fuel cells to harvest electrons from their metabolic activities.<sup>30,31</sup> The EET-based device used for harvesting energy is called “microbial fuel cell” (MFC). MFC is proposed as an attractive renewable energy source because of its ability to convert organic waste into electricity, which has demonstrated promising performance in wastewater treatments. Additionally, MFCs can also be configured as biosensors to detect aquatic toxic compounds and monitor water quality.<sup>32</sup> These MFC-based biosensors are commonly employed in wastewater treatment plants to detect the presence of high concentration organic contaminations or toxic compounds (e.g. heavy metals or pesticides). Different types of MFCs along with their working principles have been extensively investigated in the last decades.<sup>3,30,31,33–35</sup> However, most of these studies have suggested that the low power density due to low EET efficiency remains the major challenge to be solved before MFCs could be utilized as reliable power sources or biosensors.

Aside from electricity generation, electrons diverted from EABs can also reduce certain metal ions or soluble organic compounds in wastewater for resource recovery. For instance, MFCs have been used to recover biofuels (methane and hydrogen), nutrients (ammonia and phosphate), and heavy metal ions (e.g. copper, lead, cadmium, zinc, nickel).<sup>4,31</sup> However, the real-world application of this technology is restricted by its high cost and technical difficulty for recovery from rarely concentrated sources. Improving the EET efficiency to enhance the recovery performance is considered as the key to overcome these limitations.

In addition, EET is recently gaining increasing recognition for its potential applications in bioelectronics field. In particular, the protein-based, biosynthetic EET components are being exploited as conductive building blocks for next-generation bioelectronic devices such as biosensors, bio-transistors, and bio-capacitors.<sup>5,36</sup> The nontoxic, room temperature, and water-based production of these genetically encoded, electroactive biomaterials differs substantially from that of traditional synthesis/fabrication strategies. More importantly, they provide the unique potential to mediate the intrinsic biophysical and biochemical mismatches between biological systems and artificial electronics for a range of bio-interfacing applications including biomedical sensing, prosthetics, and bio-computation. However, compared with conventional electronic materials such as metals, semiconductors and conductive polymers, the conductivities of these biosynthetic materials are significantly lower, thus improving their electrical properties would be critical for their eventual utilization in bioelectronic applications.<sup>34</sup>

In short, EET has demonstrated outstanding potentials in many fields, including energy generation, resource recovery, and bioelectronics. However, EET’s low efficiency remains a major challenge that hinders the developments of its applications, thus presenting an urgent need for researchers to better understand the fundamental mechanisms of EET so as to identify and address the key limiting factors. Therefore, tools that could seamlessly interface with EET at relevant length scales are highly demanded. The

1 emerging nano- and micro-technology can be very unique <sup>26</sup>  
 2 probing and controlling the molecular- through cellular-level <sup>27</sup>  
 3 processes. In next section, we will critically review the recent <sup>28</sup>  
 4 progresses in the design and application of these small-scale tools <sup>29</sup>  
 5 for EET studies that have yielded biological insights that would have <sup>30</sup>  
 31

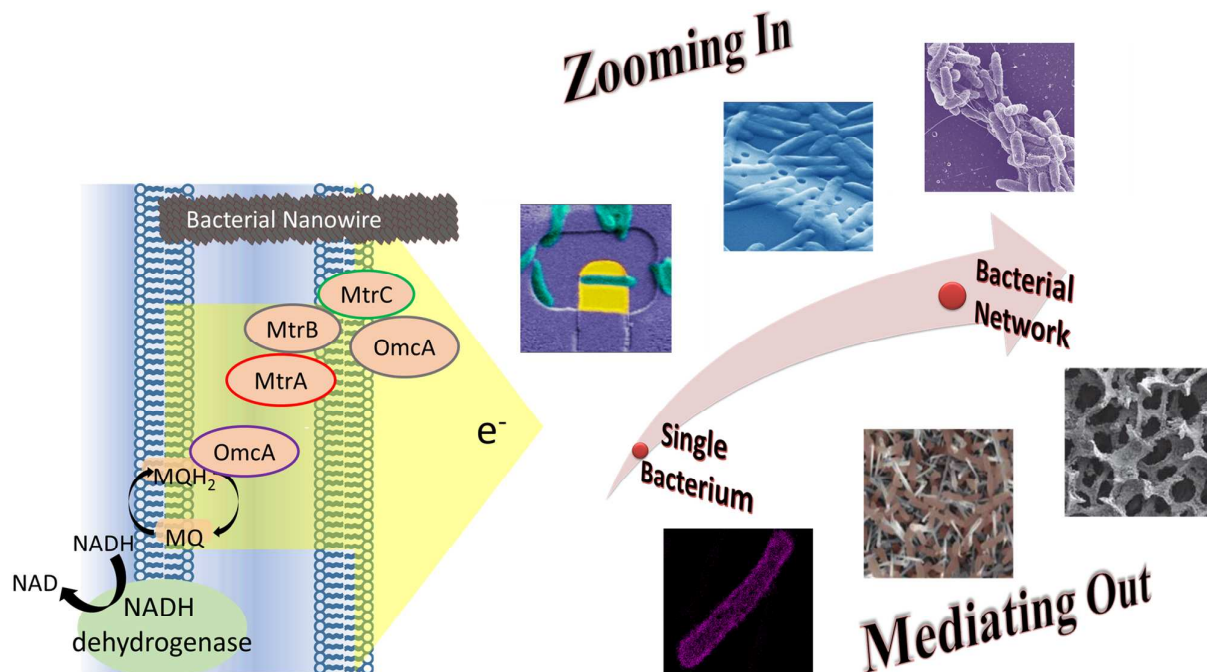


**Fig. 1** Scheme of nanotechnology enabled EET based mechanism studies and efficiency elevations in a rationally-designed, synthetic ecosystem across different length scales: from single bacterium current generation, to bacterial-electrode interaction, and eventually to bacteria-bacteria EET and network level. Reprinted with permission from ref. 45, 69 (Copyright 2018, Wiley-VCH), 81 (Copyright 2014 American Chemical Society), 87 (Copyright 2018 American Chemical Society), 91 (Reproduced permission from The Royal Society of Chemistry).

6 been inaccessible through traditional population-level experiments <sup>32</sup>

### 7 III. Nanotechnology Enabled EET Investigation <sup>33</sup>

8 In native biofilm, EABs' cellular materials (e.g. cytoplasm, outer <sup>35</sup>  
 9 membrane etc.) and their self-assembled electroactive components <sup>36</sup>  
 10 in extracellular polymeric substances (EPS) serve as basic building <sup>37</sup>  
 11 blocks to construct various electron transfer pathways for long- <sup>38</sup>  
 12 range EET. Most of these EET components demonstrate <sup>39</sup>  
 13 conductivities in the range  $10^{-9}$  S $\cdot$ cm $^{-1}$  to  $10^3$  S $\cdot$ cm $^{-1}$ . <sup>40</sup> Outer <sup>41</sup>  
 14 membranes play a key role in transferring intracellular metabolic <sup>42</sup>  
 15 electrons to terminal electron acceptors, and could also function <sup>43</sup>  
 16 as intermediate conduits in long-range charge transport. Outer <sup>44</sup>  
 17 membranes of *Shewanella* and *Geobacter* are mainly consisted <sup>45</sup>  
 18 of cyts that have been systematically studied and summarized <sup>46</sup>  
 19 in Section II. Nevertheless, the comprehensive understanding <sup>47</sup>  
 20 of extracellular charge transport is still limited by the complexity <sup>48</sup>  
 21 of EPS that contains proteins, nucleic acids, humic substances, lipids <sup>49</sup>  
 22 and BNWs. Many efforts have been made to investigate the <sup>50</sup>  
 23 functions of each component in the EET processes. In particular, <sup>51</sup>  
 24 different types of BNWs have been found to be directly associated <sup>52</sup>  
 25 with biofilm conductivities <sup>37</sup>. Scanning tunnelling microscopy <sup>15</sup> and

are investigated via two-terminal current-voltage measurements <sup>32</sup>  
 with fabricated nanoelectrodes. Based on these measurements, the <sup>33</sup>  
 conductivity of *Shewanella*'s BNWs is determined to be in the range <sup>34</sup>  
 of  $60$  (mS $\cdot$ cm $^{-1}$ ) to  $1$  (S $\cdot$ cm $^{-1}$ ), <sup>38</sup> whereas that of *Geobacter*'s BNWs <sup>35</sup>  
 is within  $51 \pm 11$  (mS $\cdot$ cm $^{-1}$ ). <sup>39</sup> These measurements strongly indicate <sup>36</sup>  
 that BNWs are not the only factors determining the overall EET <sup>37</sup>  
 efficiencies since their conductivity is sufficient to discharge the <sup>38</sup>  
 entire electrons generated from metabolism of a single EAB ( $10^6$  <sup>39</sup>  
 electrons per cell per second) to electron acceptors. <sup>40</sup>

While these ex-situ, "top-down" strategies have provided important <sup>41</sup>  
 insights about charge transport within isolated, fixed EET "modules," <sup>42</sup>  
 the ultimate understanding of EET needs to be placed in the context <sup>43</sup>  
 of relevant microenvironment where EET occurs. When the local pH <sup>44</sup>  
 increases from 2.7 to 10.5, for instance, *Geobacter*'s BNWs' <sup>45</sup>  
 conductivity decreases from  $188 \pm 34$  (mS $\cdot$ cm $^{-1}$ ) to  $37 \pm 15$  (mS $\cdot$ cm $^{-1}$ ). <sup>46</sup>  
 A "bottom-up" paradigm is recently emerging, where <sup>47</sup>  
 nanotechnology-enabled platforms are being developed to <sup>48</sup>  
 rationally engineer and probe individual cells, their local <sup>49</sup>  
 environments and cellular interactions to provide more <sup>50</sup>  
 comprehensive and biologically relevant information about native <sup>51</sup>  
 EET. Different from the aforementioned top-down approaches, it <sup>52</sup>

1 represents a unique strategy to precisely interpret and interrogate 28  
2 key steps of the entire EET process in a rationally-designed 29  
3 synthetic ecosystem: from single bacterium current generation, 30  
4 bacterial-electrode interaction, and eventually to bacteria-bacterium 31  
5 EET and network level performance (Fig. 1). From these studies, 32  
6 sophisticated EET model can be built to comprehensively illustrate 33  
7 the cascade of electron transfer processes. Currently, these 34  
8 approaches have provided unambiguous insights into single 35  
9 bacterium's EET efficiency and also revealed key factors 36  
10 bacterium-electrode and bacterium-bacterium interactions that 37  
11 play critical roles in determining the overall EET efficiency. 38  
12 **A. Single cell measurement** 39  
13 The heterogeneity of biofilm introduces numerous variations in the 40  
14 populational level studies of the bacterial behaviours which can be 41  
15 overcome by precisely probing cellular dynamics at single bacterium 42  
16 level.<sup>40,41</sup> In the context of EET, probing the electrochemistry at 43  
17 single EAB level with precisely modulated microenvironments and 44  
18 bacterium-electrode contacts can help unravel the heterogeneity 45  
19 and complexity in biofilm-level measurement, thus unambiguously 46  
20 determining the fundamental limits and mechanisms of EET. Micro- 47  
21 /nano-fabricated electrodes, with dimension comparable to 48  
22 individual EABs, have been demonstrated as powerful tools to 49  
23 analyse cross-membrane EET at single-bacterium level. Jiang et al. 50  
24 report the first single-bacterium level electrochemical study of 51  
25 *Geobacter sulfurreducens* DL-1 using optically transparent 52  
26 microelectrode arrays confined in separated microchambers.<sup>42</sup> (Fig. 53  
27 2 (a) insert) This device allows localized current recordings from 54  
55  
56 multiple electrodes within a controlled microenvironment.  
Measurements are initiated by injecting DL-1 into the device. Two  
hours after the injection, all recorded currents of four electrodes (in  
two separated wells) show stepwise increases (Fig. 2 (a)). Each  
current increase consists of two processes: an initiation by a fast-  
decaying peak attributed to the quick discharge from the cell  
membrane with accumulated electrons, followed by a stable  
plateau corresponding to sustained cross-membrane EET from DL-1.  
The multiplex recordings suggest that these current increases are  
localized to individual electrodes and directly associated with the  
bacteria-electrode contacts. This conclusion is supported by the  
simultaneous electrical recording and optical imaging, which  
demonstrate that the recorded current increased to ~ 82 fA (Fig. 2  
(b) top) immediately after single DL-1 makes a physical contact with  
the electrode surface. Furthermore, the contact of a two-bacterium  
assembly with measured electrode leads to a larger current  
increase of ~ 185 fA (Fig. 2 (b) bottom), showing that the current  
amplitude is determined by the number of DL-1s that are involved  
in the interaction. Besides, the long range direct EET can also be  
detected by this platform. As presented in the long-term  
measurements, a dramatic rise (more than 5 folds) of recorded  
current is observed when a close packed network is formed. It is  
noteworthy that the change in bacterial number on measured  
electrodes (7-to-10 and 6-to-8) is negligible compared with the  
magnitude of current increasing. These results indicate that this  
dramatic current increase does not only originate from direct  
bacteria-electrode interactions but also from the surface protein  
and/or BNW-enabled long-range EET in the developed DL-1  
network.

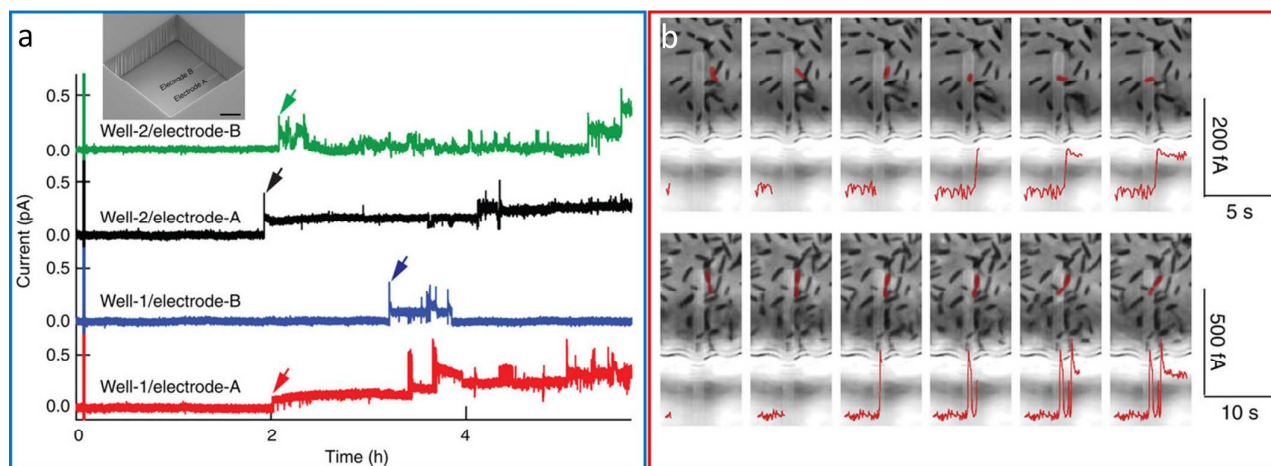


**Fig. 2** Multiplex electrochemical measurements of *Geobacter sulfurreducens* DL-1 at single bacterium level.<sup>42</sup> (a) EET current recording on four selected electrodes in two isolated wells. Recording is started immediately after bacteria introduction; the red, blue, black and green arrows mark the occurrence of the first current step on each electrode at  $\sim 1$  h after inoculation; inset: SEM image of a pair microelectrodes in microwell for EET current recording and (b) Evolution of in situ phase-contrast images of DL-1 cells on and around the measured electrode when a 82-fA (one bacterium contact) (top) and 185-fA (multi-bacteria contact) (bottom) current spike is recorded, respectively. Reprinted with permission from ref. 42.

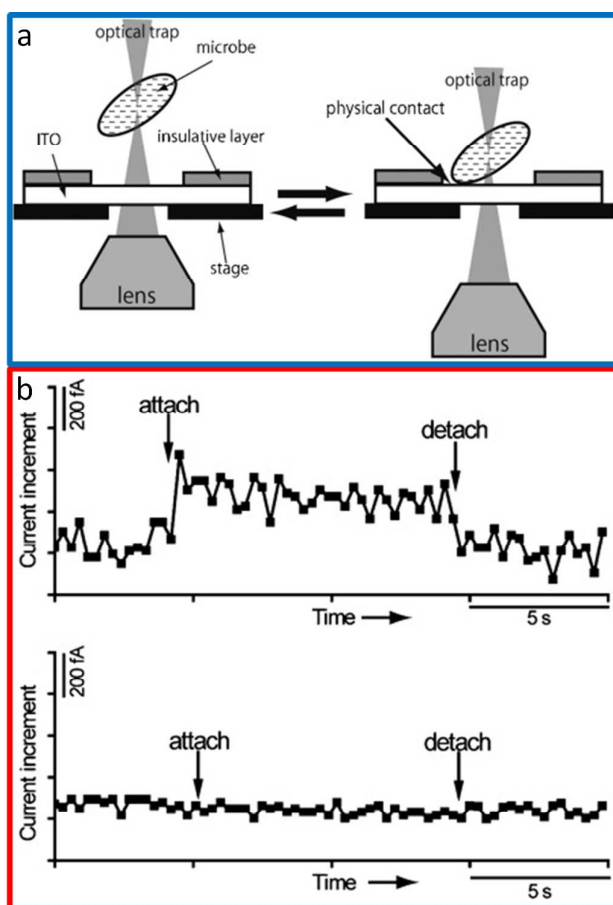


**Fig. 3** Single *Shewanella loihica* PV-4 measurement. (a) Schematic of EET measurement platform with incorporated optical tweezer and microelectrode; and (b) short circuit current measurements when (b1) wild type PV-4 and (b2) PV-4 with reduced amount of surface cyts attached to and detached from microelectrodes. Reprinted with permission from ref. 43. Copyright 2010, Wiley-VCH

1 Compared with *Geobacter* which has only been associated with

2 direct EET mechanisms, *Shewanella* can perform both direct and  
 3 indirect cross membrane EETs, making the investigations more  
 4 complicated. Liu et al. develop a platform that combines an optical  
 5 tweezer and a micropatterned ITO electrode to access the EET  
 6 current generated by single *Shewanella loihica* PV-4, where the  
 7 current generation can be studied in the context of single  
 8 cell/electrode interaction and constant electron mediator  
 9 background.<sup>43</sup> In particular, motions of single PV-4 can be  
 10 manipulated by an optical tweezer generated by focusing a Nd:YAG  
 11 laser (2 mW, wavelength = 1064 nm) through a 100 X oil-immersion  
 12 objective lens. By moving the objective lens vertically, the optically  
 13 trapped PV-4 can be attached to and detached from the ITO  
 14 electrode (Fig. 3 (a)). The electrochemical current between PV-4  
 15 and ITO (poised at 0.2V) is continuously measured under strict  
 16 anaerobic conditions to eliminate the influence from O<sub>2</sub>. During the  
 17 measurement, the stable background current can be recorded  
 18 when PV-4 is detached from ITO. Moving PV-4 to physically contact  
 19 the ITO electrode leads to a rapid increase in the measured current  
 20 (Fig. 3 (b)). This current is stabilized at certain point during PV-4-  
 21 electrode contact, which is attributed to the constant respiratory  
 22 electron output from PV-4. After detaching PV-4 from the ITO  
 23 electrodes, the measured current immediately reduces to its  
 24 background level. The EET current of single PV-4 can thus be  
 25 calculated at approximately 200 fA by subtracting the background  
 26 current from the current recorded during PV-4-electrode contact  
 27 (Fig. 3 (b) top). In a separate measurement, PV-4 with reduced  
 28 amount of surface cyts cannot generate similar response (Fig. 3 (b)  
 29 bottom), which further demonstrates that the current increase  
 30 during PV-4 attachment is originating from the surface protein  
 mediated direct EET.

These single-bacterium measurements also enable the estimation  
 of the intrinsic limit of MFC current density, which could be  
 calculated by dividing single DL-1 or PV-4 current outputs by the

1 physical volume of EAB. This estimation gives a value of  $10^6$  (A/m<sup>2</sup>)  
2 which is 2–3 orders of magnitude higher than the best volumetric  
3 current density reported in working MFCs.<sup>44</sup> This estimation  
4 indicates that the low performance of most EET implications is not  
5 restricted by the cross membrane EET efficiencies of EABs but  
6 rather by other factors including longer range charge/mass  
7 transport at network levels.

8 EABs can interact with electrodes through both direct (physical  
9 contact) and indirect (mediator) EETs. A detailed understanding of  
10 EAB-electrode interactions and how these processes are translated  
11 into current generation can provide important insights into  
12 improving EET efficiency at this heterogeneous interface; however,  
13 the limitations posed by conventional EET measurement techniques  
14 still challenge the deconvolution of these mechanisms. To address  
15 these challenges and better understand the fundamental electro-  
16 transfer mechanisms between EABs and electrodes, Jiang et al.  
17 have developed a nanoscale measurement platform which allows  
18 accurate control of physical contacts between individual bacterium  
19 and electrodes,<sup>45</sup> enabling unambiguous differentiation between  
20 these two mechanisms. This platform consists of two types of  
21 nanostructured electrodes covered by a silicon nitride passivation  
22 layer. To regulate the EAB/electrode contact, this silicon nitride  
23 layer is patterned by e-beam lithography and reactive ion etching  
24 comprise either 150 nanohole (200 nm × 400 nm) array or single  
25 micro-window (6 μm × 10 μm) openings (Fig. 4 (a)). Both  
26 *S. oneidensis* MR-1 and *G. sulfurreducens* DL-1, two model EAB  
27 systems, have been studied using this platform. As presented in the  
28 SEM images (Fig. 4 (b)), during the measurement, bacteria on the  
29 nanoholes are prohibited from direct physical contact with the  
30 electrode; therefore, electrons can only be transferred by diffusible  
31 mediators. Alternatively, both mediators and surface cyts can  
32 contribute to the EET processes of bacteria which are in contact  
33 with micro-window electrodes. Short-circuit current (vs. Ag/AgCl  
34 reference) on both types of electrodes is recorded to quantitatively  
35 differentiate the contribution of direct EET mechanism from that of  
36 mediated EET mechanism. During *S. oneidensis* MR-1 measurement,  
37 both nanohole and micro-window electrodes reach a steady state  
38 current of 5 pA within 15 min after inoculation. The in-situ phase-  
39 contrast imaging confirms that MR-1 cells do not develop contact  
40 with either electrode within this short time frame. Moreover, both

recorded currents stay constant during 50 min recording period,  
despite the increasing amounts of bacteria that are in contact with  
micro-window electrode after 20 min incubation (Fig. 4 (c)). These  
observations suggest that physical contacts between bacteria and  
electrode are not essential in early stage EET of MR-1. In longer  
term short-circuit current measurement after biofilm formation,  
micro-window electrode still records similar level of current as  
nanohole electrode. Furthermore, both electrodes respond similarly  
to the removal and re-introduction of mediators which lead to 95%  
reduction and 80% recovery of EET currents, respectively. These  
results indicate that mediator-driven indirect EET plays the major  
role in EET of MR-1. As a comparison, in the long-term  
measurement of *Geobacter* DL-1, current generation can only be  
observed on the micro-window electrode within the first 8h,  
indicating the electron transfer of DL-1 is dominated by the direct  
EET at the initial stage (Fig.4 (d)). Overall, this nanotechnology-  
based platform consisting of engineered nanoelectrodes and in situ  
optical imaging represents a unique tool to unambiguously address  
the fundamental mechanisms of EET in the context of EAB-  
electrode interactions.

## B. EET Study at Network Level

Native EAB biofilms grown on solid-phase electron acceptors, such  
as MFC anodes, are usually tens of micrometers in thickness. As a  
result, the majority of bacteria have to perform long range EET to  
remotely “dump” the respiratory electrons and complete the  
metabolic cycle. Hence, a better understanding of inter-cellular EET  
is ultimately central to understanding the performance of  
bioelectrochemical systems at ensemble level. Furthermore, this  
knowledge can create the possibilities to manipulate the EET  
process for applications beyond energy harvesting (e.g.  
bioelectronics and biocomputing). Technically network-level EET  
investigation has been mainly challenged by the intrinsic complexity  
of native biofilm which contains a heterogeneous mixture of EABs  
and EPS components (such BNWs, polysaccharides, humic  
substances etc.) with a broad spectrum of electrical properties.<sup>34</sup>  
The recent development and application of nano- and micro-  
technology has opened up new possibilities to overcome these  
challenges, in which the cellular interaction, microenvironment and  
local electrochemistry can be rationally controlled to precisely  
construct and interrogate EET pathways at a range of length scales.

1 Malvankar et al. design a platform which contains a pair of gold  
2 electrodes separated by a non-conductive gap of 50  $\mu\text{m}$  bridged  
3 a confluent *Geobacter sulfurreducens* DL-1 biofilm. This platform  
4 allows for specific measurement of the long-range EET of DL-1  
5 situ.<sup>19</sup> Through (1) controlling the culturing conditions to regulate  
6 the development of conductive pili; as well as (2) applying the  
7 genetic engineering tool to suppress the expression of all outer  
8 membrane cty's, this platform demonstrates that the conductive pili  
9 are the most essential component to electrically bridge *Geobacter*  
10 for long range EET. Combing the results from temperature  
11 dependent conductivity measurement, Malvankar et al. propose

which one electrode with a relatively positive potential acts as  
electron source, while the other one acts as electron drain. Notably,  
the potentials of both electrodes are controlled in the range that no  
acetate oxidation can be triggered; therefore, the electron transfer  
event can only occur in the biofilm between two electrodes. The  
results of both type 1 and 2 measurements fit well with the  
multistep electron hopping numerical model. The model suggests  
that the redox gradients of biofilm are present in the vicinity of  
each electrode during both measurements. This redox gradient can  
drive electrons transport either from acetate oxidation on biofilm to  
electrode 1 (type 1) or between two electrodes (type 2). Based on

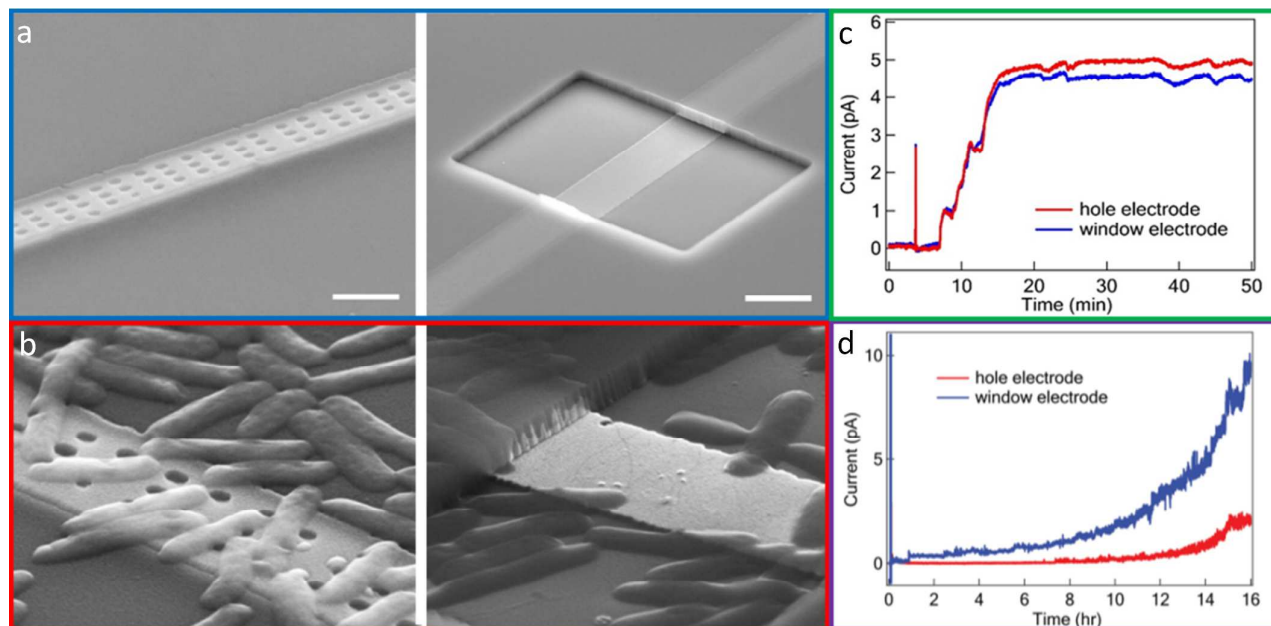


**Fig. 4** Nanostructured electrodes for probing EET. (a) SEM images of nanohole and micro-window electrodes; (b) SEM images of MR-1 on nanohole and micro-window electrodes at  $\sim 1$  h after inoculation; and long term EET current measurements of (c) MR-1 and (d) DL-1 on both nanohole and micro-window electrodes.<sup>45</sup> Reprinted with permission from ref. 45.

12 “metallic-like” EET mechanism of *Geobacter* network that  
13 electrons are delocalized and move through the  $\pi$ -conjugated  
14 aromatics across the bacterial network.

these results, Snider et al. propose a multi-site electron hopping  
mechanism that the EET of DL-1 network is driven by the redox  
gradient between electron donors and acceptors.

15 Alternately, Snider et al. study the long-range EET within *Geobacter*  
16 *sulfurreducens* DL-1 biofilm grown on an interdigitated  
17 microelectrode array (IDA). This IDA contains 2 interdigitated  
18 electrodes (electrode 1 and 2, each comprised of 50 microelectrode  
19 bands) with 15  $\mu\text{m}$  separations between adjacent pair.<sup>46</sup> After  
20 biofilm growth under biased potential at 0.300 V (vs. Ag/AgCl), two  
21 types of electrochemical studies are performed. In the first type,  
22 the potential applied to electrode 1 is swept from 0.300 V to -0.750  
23 V which continuously performs as the only EET terminal to accept  
24 the electron generated by acetate oxidation on the biofilm.  
25 Simultaneously, the open circuit potential of electrode 2 is  
26 measured, which indicates the oxidation state of the biofilm. In the  
27 second type, potentials of both electrode 1 and 2 changes during  
28 measurement while maintaining a constant (0.1 V) potential  
29 difference. This potential difference establishes an EET pathway  
30 across the 15  $\mu\text{m}$  biofilm between each adjacent electrode pair

Moreover, Ding et al study the EET mechanisms in both *Shewanella*  
*oneidensis* MR-1 and *Geobacter sulfurreducens* PCA networks using  
a customized microelectrode array which contains paired  
microelectrodes with various surface areas and separations.<sup>47</sup> In  
two terminal current-voltage measurement with the applied  
potential from -0.2 V to 0.2 V, the response currents across both  
EABs are independent of the electrode separations but strongly  
correlated with the electrode areas (Fig. 5 (a)), thus suggesting that  
the measured EET is dominated by the electrochemical reactions at  
the bacteria-electrode interfaces. To independently detect the  
electrochemical (from EABs to counter electrode) and electron  
transfer (across EAB bridged pair electrodes) components of this  
system, electrical transport spectroscopy (ETS) is carried out on MR-  
1 biofilm as a model system. In the ETS studies, the counter  
electrode functions as a gate electrode (similar to the conventional  
field effect transistors), and the reference electrode (Ag/AgCl) is

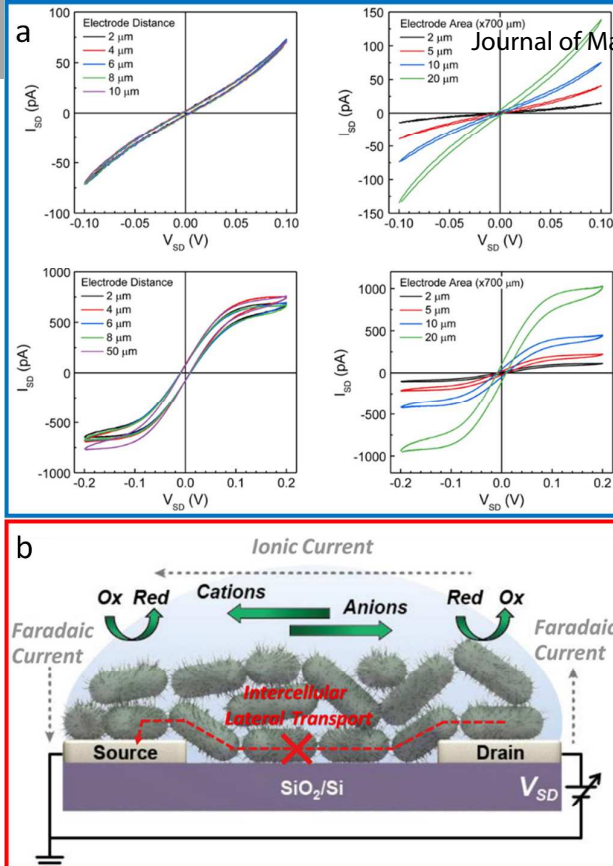


**Fig. 5** On-chip nanoelectronic investigation of EET. (a) two terminal I-V measurements of *Shewanella oneidensis* MR-1 and *Geobacter sulfurreducens* PCA on microelectrode arrays with different electrode areas and electrode distances; and (b) schematic of the electrochemical-reaction dominated EET mechanism proposed by Ding et al. Reprinted with permission from ref. 47. Copyright 2016 American Chemical Society

1 used to regulate the electrical potential applied on the EABs. The  
 2 measured electrochemical currents and the electron transfer  
 3 currents exhibit comparable amplitudes which indicate that the  
 4 measured electron transfer process is closely correlated with  
 5 electrochemical reactions. Based on these results, Ding et al.  
 6 introduce an alternative model to explicate the EET mechanisms  
 7 (Fig. 5 (b)) that the electron transfer is determined by the  
 8 electrochemical reactions at the bacteria-electrode interface. In this  
 9 model, the direct electron transfers across biofilms does not exist,  
 10 whereas, the EET is completed by coupling the electrochemical  
 11 reactions at both terminals of biofilms through liquid phase ionic  
 12 charge transfer.

13 Overall these customized microelectrode platform enables electron  
 14 transfer measurement with controlled electrochemistry and

5 bacteria-electrode interactions. The discrepancy between their  
 6 conclusions, however, indicates the intricacy of long-range EET  
 7 mechanisms which could be further complicated by the  
 8 heterogeneity of EAB biofilms. Hence, there is a strong need to  
 9 further optimize these EET studies by establishing a rationally  
 10 designed bacterial network where microenvironments and  
 11 bacterium-bacterium interactions can be precisely manipulated.  
 12 This effort can potentially lead to a full understanding of structure-  
 13 function correlation in the context of bacterial interactions to  
 14 unambiguously elucidate the underlying EET mechanisms in the  
 5 bacterial networks.

#### 6 IV. Nanostructured Materials for Facilitating EET

7 EET performed by electrochemically active bacteria, though holding  
 8 tremendous potentials, still has limited efficiency. This challenge  
 9 posed by the natural EET process is hindering most downstream  
 10 applications such as energy conversion and resource recovery. For  
 11 example, a combination of hydrodynamic experiments and  
 12 numerical modelling of the response of *G. sulfurreducens* biofilms  
 13 cultured on a rotating disk electrode demonstrate that the cells  
 14 furthest from the electrode are limited by the rate at which  
 15 electrons could be transported through the extracellular matrix and  
 16 are determined to be respiring close to their basal metabolic rate.<sup>48</sup>

17 Nanoscale materials, such as metal/semiconductor nanoparticles  
 18 and carbon nanotubes, have been extensively studied to promote  
 19 electron transfer in bioelectrocatalysis.<sup>49</sup> The electron transfer rate  
 20 in amperometric biosensors or enzymatic fuel cells, for example,  
 21 has been found to be significantly improved by incorporating  
 22 nanostructures that allow for optimal alignment of  
 23 bioelectrocatalysts and thus more effective coupling with active  
 24 redox centres.<sup>50-53</sup> For EABs, the whole bacterium, instead of  
 25 individual biomolecules, is involved in biocatalytic process;  
 26 nonetheless the charge transport is fundamentally carried out  
 27 through EET-specific molecules/molecular assemblies thus could  
 28 also benefit from similar approaches. In this part, we will present  
 29 and critically discuss the research strategies that have been  
 30 developed to utilize rationally designed and integrated  
 31 nanomaterials for EET facilitation at both EAB/electrode and  
 32 EAB/EAB interfaces.

#### 33 A. Facilitating EET at EAB/Electrode Interface

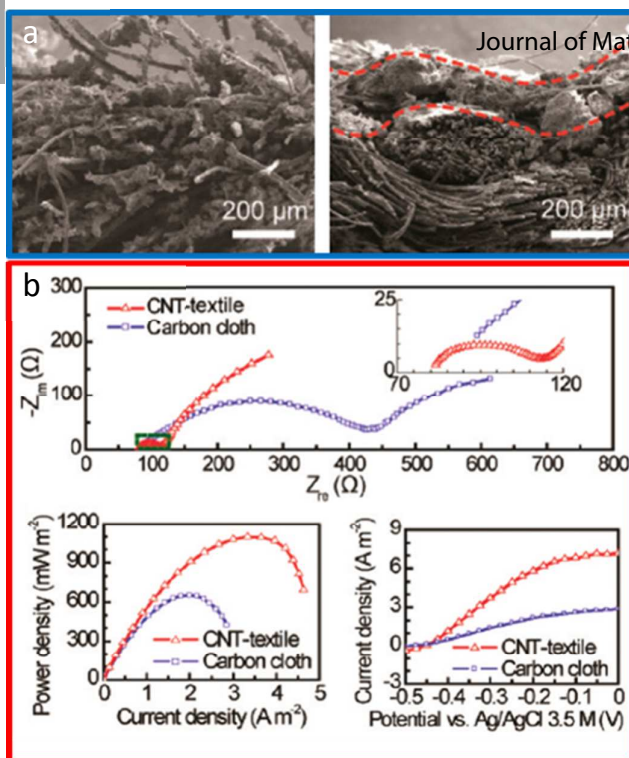


**Fig. 6** CNT-textile anode enabled MFC performance improvement. (a) SEM images of the bacteria growth on the CNT-textile (left) and the carbon cloth (right) anodes and (b) Performance of MFCs equipped with CNT-textile and carbon cloth anodes. Reprinted with permission from ref. 54 Copyright 2011 American Chemical Society

As the terminal electron acceptors for many EET applications, electrodes, particularly their interfaces with EABs, are playing critical roles in determining the overall device performance. However, several intrinsic mismatches in biophysical/biochemical properties between bacteria and conventional electrode materials restrict the EET efficiency at these biotic-abiotic interfaces. With rationally designed structure and physical/chemical properties, bottom-up synthesized nanomaterials hold great promise for overcoming this barrier. Below we will discuss several strategies that have been exploited for electrode modification to facilitate the electron exchange with EABs.

## ARTICLE

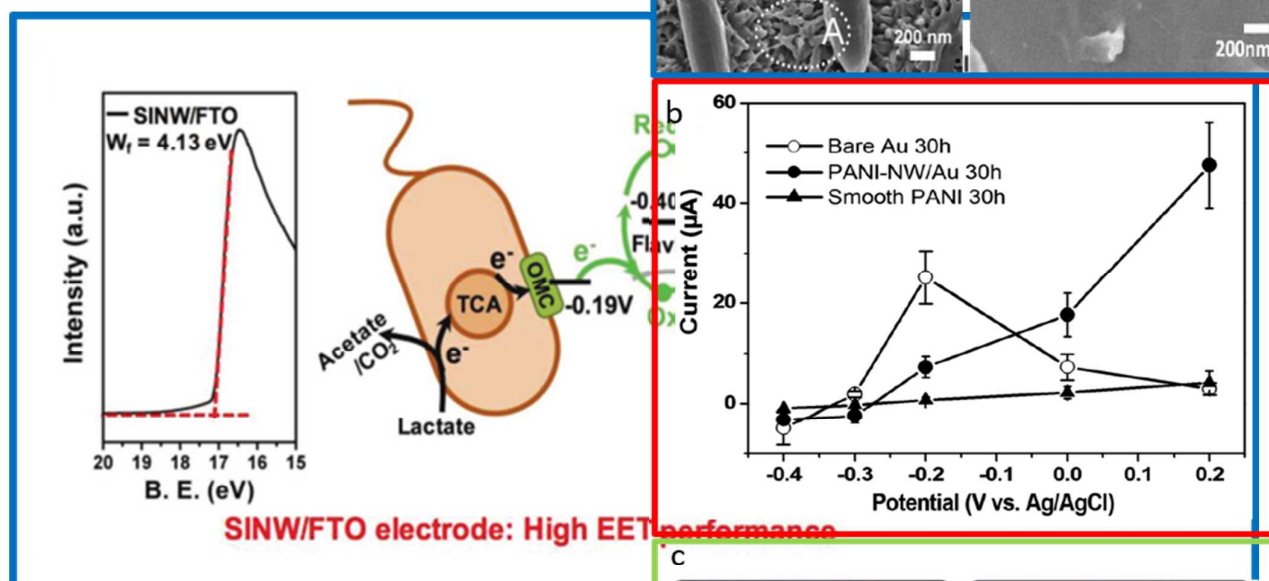


**Fig. 8** SINW/FTO electrode for facilitating both direct and indirect electron transfer. (a) SEM images of cells on a PANI-NA/Au electrode (left) and smooth electrode (right); (b) Influence of poised potentials on EET currents on PANI-NA/Au (solid circles), smooth PANI/Au (solid triangle) and bare Au (open circles) electrodes; (c) Schematic of bacterial EET on a PANI-NA/Au electrode under different poised potentials. Reproduced from Ref. 61 with permission from the Royal Society of Chemistry

1 Traditional MFC electrodes (mostly carbon-based) usually involve  
 2 designs that feature increased surface area (e.g. carbon cloth,  
 3 graphite brush, stainless steel brush, carbon paper etc.) to reduce  
 4 the contact impedance with EABs. Recently Xie et al. have  
 5 developed a porous, hierarchically structured anode comprising  
 6 woven polyester fibers with conformally coated CNTs to further  
 7 improve the power extraction.<sup>54</sup> In this anode, macro-pores provide  
 8 3D openings which allow bacteria to form biofilm inside the space.  
 9 In comparison with traditional 2-D electrode, the biofilm developed  
 10 on this CNT-textile 3-D scaffold features 10-folds improvement in  
 11 the ion-biofilm-anode interfacial area for better mass transport (Fig.  
 12 6 (a)). The nanostructured CNT surface also creates additional  
 13 roughness, providing strong mechanical binding between the  
 14 developed biofilms and electrodes. These improvements lead to  
 15 90% reduction of internal resistance (30  $\Omega$  v.s. 300  $\Omega$ ) and  
 16 significantly improved power density (1098 vs 655  $\text{mW m}^{-2}$ )  
 17 compared with 2D electrode (Fig. 6 (b)). Moreover, other studies  
 18 have also demonstrated that CNT can trigger the structural  
 19 transformation of OMCs' porphyrin ring on *Shewanella*. The Fe  
 20 redox active centre can thus be more intimately coupled with CNT  
 21 via electron tunnelling, which leads to a 10-time increase  
 22 in bioelectrochemical systems' current generation.<sup>55,56</sup> Similar  
 23 strategies have also been explored in creating other 3-D macroporous  
 24 electrodes for various applications.<sup>57-60</sup>

25 Certain EABs have been known to secrete soluble mediators  
 26 electron "shuttles" when direct EET becomes challenging. Inspired  
 27 by this naturally developed strategy, nanomaterials with multiple  
 28 redox states have been explored by many groups to modify the  
 29 electrodes, which not only expand the electrode/bacteria contact  
 30 area but also facilitate EET as solid-state mediators. For example,  
 31 Ding et al. have generated a vertically-aligned polyaniline nanowire

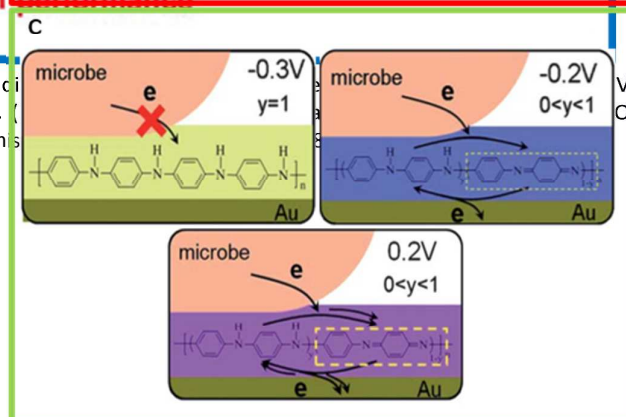
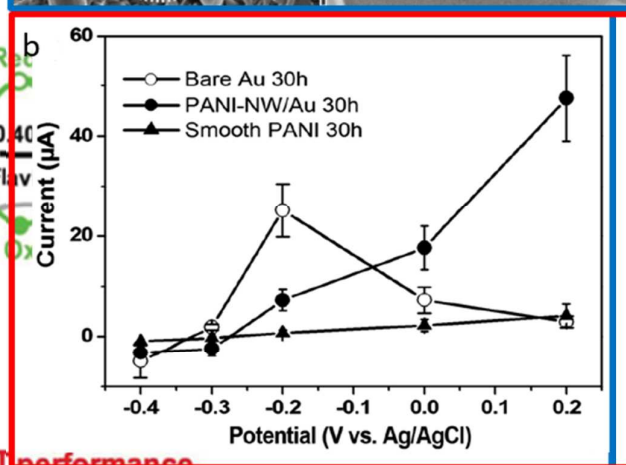
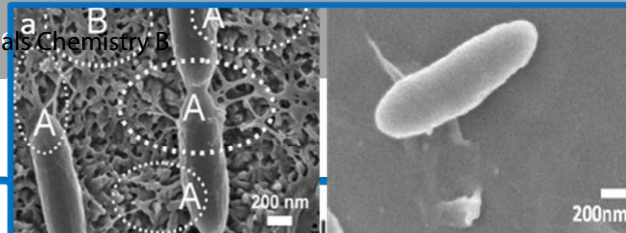


**Fig. 7** PANI-NA electrode mediated EET. (a) SEM images of cells on a PANI-NA/Au electrode (left) and smooth electrode (right); (b) Influence of poised potentials on EET currents on PANI-NA/Au (solid circles), smooth PANI/Au (solid triangle) and bare Au (open circles) electrodes; (c) Schematic of bacterial EET on a PANI-NA/Au electrode under different poised potentials. Reproduced from Ref. 61 with permission from the Royal Society of Chemistry

array (PANI-NA) on a gold (Au) electrode.<sup>61</sup> PANI is a conductive polymer which contains alternating oxidized (quinone ring) and reduced (benzene ring) repeat units, and the ratio of these two redox contents could be tuned by externally applied potential. In this electrode design, highly-oriented 3D nanostructures of PANI-NA greatly improve bacteria-electrode adhesion through enhanced local topographic interactions (Fig. 7 (a)). Correspondingly, a 51  $\mu\text{A}$  current is recorded on the PANI-NA/Au electrode, which is over 10 and 25 times higher than smooth PANI/Au and bare Au electrode, respectively. In addition, Fig. 7 (b)&(c) show that the bacteria EET currents can be further increased by raising the applied potentials. With the positive shift of external potential, reduced units in PANI polymer chain are converted to oxidized states, which has similar function as flavin to mediate the electron transfer. This work demonstrates the possibility to improve EAB-electrode coupling through (1) promoting the physical/topological contacts and (2) tuning the interfacial redox states to reduce the charge transfer

1 barrier. Similarly, a variety of other nanomaterials have also been  
2 explored in the electrode modification to facilitate EET  
3 bacteria/electrode interface such as polypyrrole<sup>62,63</sup>, nano-  
4 structured Au/Pd,<sup>64,65</sup> TiO<sub>2</sub>,<sup>66</sup> MnO<sub>2</sub>,<sup>67</sup> and NiO<sup>68</sup> etc.

5 Besides, the rational design and tuning of materials' electronic  
6 properties offers additional possibility to bridge the energy gap  
7 EAB/electrode interface. To engineer the most efficient and  
8 compatible electrodes, the selection and modification of  
9 nanomaterials are of utmost importance. As an outstanding  
10 material candidate for this purpose, nanoscale semiconductors  
11 allow for the precise modulation of their electronic states through  
12 synthetic control. Based on this strategy, Bian et al. have come  
13 with a platform that incorporates In<sub>2</sub>O<sub>3</sub> nanowire arrays on a flat  
14 doped In<sub>2</sub>O<sub>3</sub> (FTO) electrode.<sup>69</sup> The Fermi levels of these In<sub>2</sub>O<sub>3</sub>  
15 nanowires can be tuned to a desired range by Sn doping to reduce  
16 the energy barrier at bacteria-electrode interface. In this work, the  
17 Fermi levels of Sn-doped In<sub>2</sub>O<sub>3</sub> nanowire (SINW) are set at -0.57 V  
18 to match with other electron transfer components, namely FTO  
19 (Fermi level = -0.02 V), outer membrane cytochrome (OMC) (Fermi  
20 level = -0.2V), and the electron shuttle flavin (Fermi level = -0.4 V).  
21 Consequently, under a 0.2 V potential, SINWs can effectively  
22 facilitate both direct (OMCs (-0.2V)-to-FTO (-0.02 V)-to-external  
23 potential (0.2V)) and indirect (flavin (-0.4V)-to-SINW(-0.57V)-to-  
24 external potential (0.2V)) EETs (Fig.8). Introducing additional  
25 flavin/malonic acid only effectively enhances/inhibits indirect EET  
26 process in the system equipped with SINW/FTO electrodes, which  
27 further confirms that the indirect EET is promoted by SINW. Overall,  
28 these unique properties of SINWs can lead to a 60 times  
29 enhancement in current generation as compared with that of a flat  
30 FTO electrode. Based on similar strategies, several other  
31 nanomaterials with proper Fermi levels such as  $\alpha$ -Fe<sub>2</sub>O<sub>3</sub>, goethite,  
32 and Fe<sub>3</sub>O<sub>4</sub> have also been exploited as materials suitable to modify  
33 electrode's properties to match bacteria OMCs' energy level and  
34 close the charge transfer gap.<sup>70-72</sup>

35 Moreover, aforementioned strategies can be further modified to  
36 incorporate photosensitive nanoscale semiconductors to achieve  
37 optically-regulated EET. Qian et al. have developed a  $\alpha$ -Fe<sub>2</sub>O<sub>3</sub>  
38 nanowire-based anode to enable photo-enhanced electrochemical  
39 interactions between  $\alpha$ -Fe<sub>2</sub>O<sub>3</sub> and bacteria.<sup>73</sup> Specifically, under  
40 light illumination,  $\alpha$ -Fe<sub>2</sub>O<sub>3</sub> nanowires generate photoexcited  
41 electron-hole pairs. The photogenerated holes in the valence band  
42 accept electrons from *Shewanella*, while the photogenerated  
43 electrons flow through an external circuit for cathodic reduction  
44 (Fig. 9). This effect results in a 150% increase in current density  
45 compared with the two other control setups which contain either  
46 dead- or no bacteria on the  $\alpha$ -Fe<sub>2</sub>O<sub>3</sub> anodes. Qian et al. suggest that  
47 the current enhancement is attributed to the additional redox  
48 species associated with MR-1 cells that are thermodynamically  
49 favourable to be oxidized by the photogenerated holes. In contrast,  
50 without illuminations, all three anodes (live bacteria, dead bacteria,  
51 and no bacteria) cannot generate current. These results indicate

that light can regulate the EET process by turning on and off certain  
EET pathways between *Shewanella* and  $\alpha$ -Fe<sub>2</sub>O<sub>3</sub>.

In addition, nanomaterials are also applied to facilitate resource  
recovery through enhanced electrosynthesis (reversed EET). For  
example, Nie et al.<sup>74</sup> introduce nickel (Ni) nanowires as the  
interfacing layer between *Sporomusa* biofilm and graphite  
electrode. The Ni nanowire network provides sufficient surface  
roughness and porosity to accommodate *Sporomusa* biofilm with  
higher cell density than that of the bare graphite electrode. In  
combination with the significantly increased electroactive surface  
area, the new electrode design leads to a 2.3 fold increase in bio-  
reduction rate of carbon dioxide for acetate generation and 82.14%  
of the electrons consumed are recovered in acetate. Similarly, gold,  
palladium, or nickel nanoparticles are also applied by Zhang et al. to  
assist the electrosynthesis process of *Sporomusa*, resulting in 6, 4.7  
and 4.5 fold increase in electrosynthesis rate as compared with that

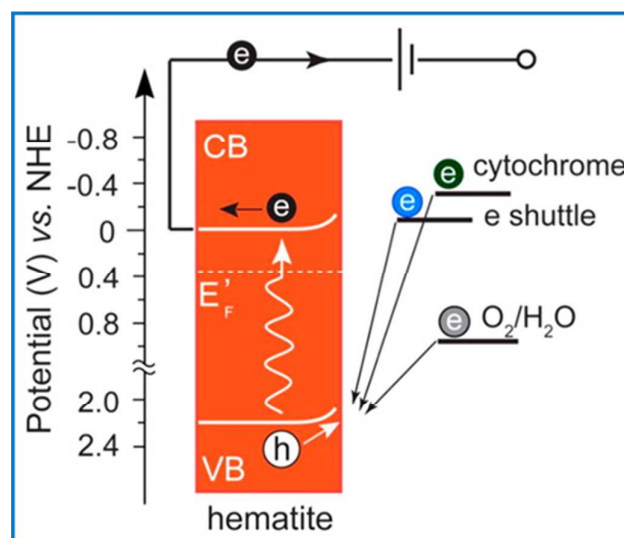


**Fig. 9** EET facilitation through photoenhanced electrochemical interactions between hematites and bacteria. Energy diagram of the  $\alpha$ -Fe<sub>2</sub>O<sub>3</sub> (hematite) photoanode in the MPS. Reprinted with permission from ref. 73. Copyright 2010 American Chemical Society

of the untreated carbon cloth electrode, respectively.<sup>75</sup>

## B. Facilitating EET at Network Level

Electrode modification with functional nanomaterials represents an effective approach to facilitate EET at EAB/electrode interface. To improve the overall EET efficiency at network level, the current strategy needs to be extended to further enhance the inter-cellular charge transport at significantly longer length scales. Thanks to their nanoscale structures and electrochemical activities, nanomaterials can be seamlessly integrated into existing EET pathways as conduits to electrically connect neighbouring bacteria to form a hybrid conductive network. This enables the linkage of electrode and distant bacteria, even the whole biofilm, to reach maximum EET efficiency.

1 For example, Zhang et al. have doped a biofilm on MFC anode with  
 2 multiwall carbon nanotube (MWCNT) to increase its EET efficiency  
 3 thus improving the power generation.<sup>76</sup> Compared with natural  
 4 biofilms, the MWCNT-doped biofilm has boosted current density  
 5 (46.2%), power density (58.8%), and coulombic efficiency (84.6%).  
 6 These results suggest that nanomaterials doping presents itself as a  
 7 promising strategy to facilitate the long-range electron transfer.  
 8 further improve the electrical coupling between EABs and inorganic  
 9 “dopants”, different strategies have been exploited to seamlessly  
 10 integrate electroactive nanomaterials into bacteria networks.  
 11 particular, EABs are known for their capability to reduce a wide  
 12 range of minerals through EET. As-formed biogenic/biomineralized  
 13 nanomaterials are highly desirable as electrical conduits since they  
 14 could naturally connect with the active redox centres of OM  
 15 which are usually wrapped by non-conductive peptide chain, thus  
 16 remaining inaccessible during conventional physical mixing  
 17 processes.<sup>77</sup> Other considerations for ideal nanomaterial conduits  
 18 include: (i) reasonably good electrical conductivity so that there is  
 19 no/little barrier for electron transfer through the nanoparticle itself  
 20 and at nanoparticle/electrode interface; (ii) appropriate  
 21 electrochemical potential so that the nanoparticle will act as  
 22 mediators instead of being terminal electron acceptor; and (iii)

good biocompatibility. Combining all these factors, iron minerals  
 stand out as the perfect materials system and have recently been  
 extensively investigated for facilitating EET at network levels.

Nakamura et al. have reported enhanced EET in *Shewanella loihica*  
 PV-4 biofilm through doping the biofilm with n-type  $\alpha$ - $\text{Fe}_2\text{O}_3$   
 nanoparticles.<sup>78</sup> According to the current measurements, after  
 completely embedding  $\alpha$ - $\text{Fe}_2\text{O}_3$  nanoparticles into PV-4 networks,  
 the EET current increases 50 times as compared with that of the  
 undoped control (Fig. 10). Also, the CV characterization clearly  
 presents a 300 time increase of peak current at OMCs redox  
 potential. These results suggest that the  $\alpha$ - $\text{Fe}_2\text{O}_3$  nanoparticles can  
 inter-connect the electron transfer pathways in the bacterial  
 network, thus promoting long-range EET processes and enhancing  
 the overall EET efficiency. Additionally, due to the unique  
 photosensitive property of  $\alpha$ - $\text{Fe}_2\text{O}_3$ , the EET efficiency in this system  
 can be further improved by diminishing the electron transfer energy  
 barrier between the *Shewanella* OMCs and  $\alpha$ - $\text{Fe}_2\text{O}_3$  through light  
 illuminations.

*Shewanella* can also reduce both elemental sulfur and subsequently  
 ferric iron to produce nanoscale mineral crusts with semiconductor-  
 like properties through biomineralization. These crusts are directly  
 coupled with the bacteria's electron transfer pathways,  
 moderating long-range electron transfer from a few bacteria to  
 external solid electron acceptors.<sup>79,80</sup> Jiang et al. have investigated  
 the detailed mechanism of nanoparticle facilitated EET in  
*Shewanella loihica* PV-4 where  $\text{FeCl}_3$  and  $\text{Na}_2\text{S}_2\text{O}_3$  are used as iron  
 and sulfur precursors to produce FeS nanoparticles at cellular  
 interfaces.<sup>81</sup> The generated FeS nanoparticles are intimately bound  
 to the bacteria membranes and interconnect to form 10–20  $\mu\text{m}$   
 sized cell/nanoparticle aggregates. (Fig. 11) In particular, EET  
 current generation is synchronized with the direct contact between  
 bacteria-FeS. aggregates and electrode which indicates that FeS-  
 EAB composites can perform the direct EET at bacteria/electrode  
 interface. Moreover, the maximum current collected from definite  
 number of bacteria/FeS aggregates (limited by the microscale open  
 window) is about 500pA which is 3 to 4 order of magnitude higher  
 than the reported values generated from single *Shewanella* or  
*Geobacter* cells. The enhancement in EET current suggests that FeS  
 nanoparticles can facilitate the long range EET by constructing an  
 electrically connected, three-dimensional cell network from  
 bottom-up. Similarly, other biogenic nanomaterials such as Au and  
 Pd nanoparticles as well as graphene oxide have also been used to  
 facilitate EET in bacterial networks.<sup>82–85</sup>

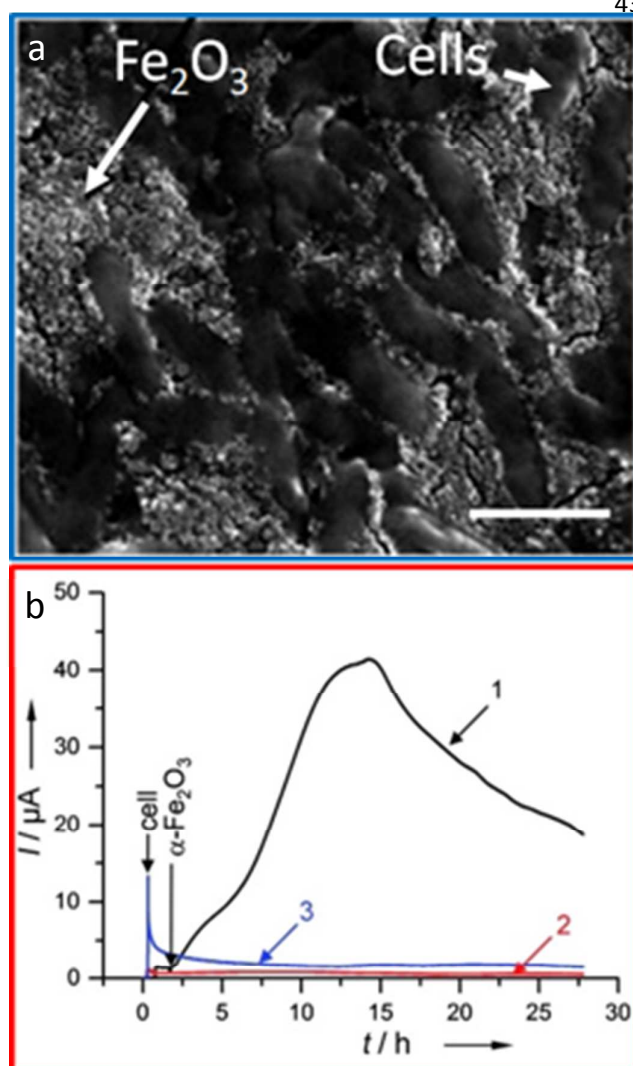


**Fig. 10** Long range EET in  $\alpha$ - $\text{Fe}_2\text{O}_3$  nanoparticle/bacteria hybrid network. (a) SEM image of the embed  $\alpha$ - $\text{Fe}_2\text{O}_3$  nanoparticles in the bacteria network. Scale bar, 2  $\mu\text{m}$ ; (b) I-t curves in the presence (trace 1), absence (trace 2) of  $\alpha$ - $\text{Fe}_2\text{O}_3$  nanoparticle and presence of  $\text{Fe}^{3+}$  (trace 3). Reprinted with permission from ref. 78. Copyright 2009 WILEY-VCH Verlag

1 In summary, this section provides an overview of diverse  
 2 nanomaterial-enabled strategies to facilitate the bacteria EET  
 3 Beyond conventional strategies that only enhance the EET  
 4 efficiencies by reducing electrode impedance, recent advances  
 5 the engineering of nanomaterial-bacteria interactions enable  
 6 rational design of effective EET pathways from bottom-up  
 7 strategies. Nanomaterials offer superb electrical properties and  
 8 tunability to reconcile the mismatches between bacteria and  
 9 electrodes. The bio-enabled synthetic process further allows for the  
 10 seamless integration of nanomaterials into existing charge  
 11 transport pathways to promote EET at network levels. Moreover,  
 12 recently, several studies demonstrate the potential of  
 13 nanotechnologies in regulating biosynthesis of extracellular  
 14 conductive materials. For example, when cultured on vertical silicon  
 15 nanowire arrays, *Sporomusa ovata* can form filamentous cells that  
 16 align parallel to nanowires with increasing ionic concentrations.  
 17 Hsu et al. create core/shell type bacteria "cables" in which the  
 18 microenvironment and cell-cell interaction can be rationally  
 19 controlled. This platform enables precise modulation of the  
 20 structural (from membrane contact to BNW connections) and  
 21 electrical properties (from 2.5 to 16.2 mS·cm<sup>-1</sup>) of the one-  
 22 dimensional conductive matrices generated by *Shewanella loihica*  
 23 PV-4.<sup>87</sup> Moreover, Zhou et al. report that the introduction of TiO<sub>2</sub>  
 24 nanoparticles during the culture of *Geobacter sulfurreducens* PCA  
 25 can promote BNW formation, and the 2.7-fold increase in PilA  
 26 protein expression can be directly translated to the improved  
 27 EET.<sup>88</sup> Overall, these studies provide valuable insights into the  
 28 rational design and production of biosynthetic electroactive  
 29 materials which pave the way for their future bioelectronic  
 30 applications. Based on these progresses, future developments in  
 31 nanomaterial-bacteria hybrid systems are expected to elevate EET  
 32 efficiencies to a completely new level, which will open up ample  
 33 possibilities in the bioenergetic, bioelectronic, and other related  
 34 research areas.

### 35 Conclusions and Future Outlooks

36 To summarize, nanotechnology-enabled platforms have been  
 37 shown to allow for the rational customization of bacterial EET  
 38 processes from bottom-up. These platforms have enabled  
 39 researchers to precisely interrogate EET from single bacterium to  
 40 network levels, providing critical insights into the fundamental  
 41 mechanisms of EET that are difficult to achieve via population-level  
 42 experiments. Furthermore, the rational design and integration of  
 43 functional nanomaterials into the bacterial EET pathways can  
 44 mediate the charge transport at both EAB/electrode and EAB/EAB  
 45 interfaces, thus significantly enhancing the EET efficiency across  
 46 multiple length scales. These efforts are advancing the  
 47 understanding of energy metabolism and electron transfer in  
 48 biological systems. Furthermore, the bacterium-nanomaterial  
 49 hybrid systems allow seamless electrical contacts and matching  
 50 energy levels at both bacterium-electrode and bacterium-bacterium  
 51 interfaces. These strategies significantly improve the EET  
 52 efficiencies, which lead to 40% to 200% increases in power

generation from that of traditional MFCs. However, some studies  
 indicate that nanomaterials could introduce unfavorable impacts to  
 EABs. Maurer-Jones et al. suggest that the gene expression of  
*Shewanella oneidensis* is changed after exposure to TiO<sub>2</sub>  
 nanoparticles. This effect not only significantly slows the biofilm  
 development but also alters the EET of *S. oneidensis* toward the  
 mediator (flavin) driven process.<sup>89</sup> More generally, several  
 nanomaterials, such as carbon nanotube and (small, <10 nm) gold  
 nanoparticles, are known to be cytotoxic.<sup>90</sup> Systematic studies of  
 the influence of these nanomaterials to EAB physiology will be  
 critical to provide important guidance in nanomaterial design and  
 selection to optimize the EET efficiency without compromising the  
 normal biological functions of EABs.

Moving forward, the fundamental EET elements, cyts, and their self-  
 assembled materials stand out as a completely new category of  
 biosynthetic electroactive materials with genetically encoded  
 properties. The inherent conductivities of these materials can  
 effectively mediate the electrical communications between biotic  
 and abiotic systems. Their protein-based nature offers inherent

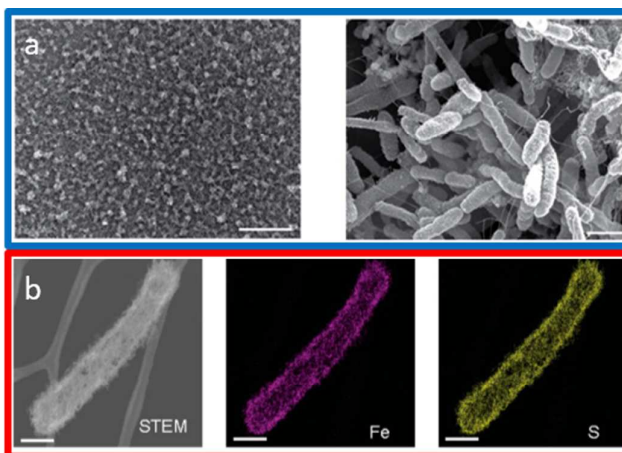


**Fig. 11** Biogenic FeS nanoparticles enhance EET. (a) SEM image of FeS/bacteria aggregate under low and high magnifications. Scale bars, 100 μm (left) and 1 μm (right). (b) Bright-field STEM image and corresponding elemental mapping of a PV-4 cell coated with nanoparticles. Scale bar, 500 nm. Reprinted with permission from ref. 81. Copyright 2014 American Chemical Society

biocompatibility as compared with traditional electronic materials  
 such as metal, semiconductors and conductive polymers, making  
 them uniquely qualified for many bio-interfacing applications.  
 However, since the development of biofilm is uncontrolled, native  
 cyt-based materials are intrinsically heterogeneous in terms of  
 structures, compositions, and electrical properties. These  
 complexities greatly challenge the structural design and fabrication  
 processes, which demands the development of nano-manufacturing  
 methods that allow precise control of the biosynthetic process to  
 produce functional biomaterials with highly purity and rationally  
 designed properties.

- 1 Overall, the integration of nanotechnology with biological  
2 systems offers tremendous opportunities in tackling both the  
3 fundamentals and applications of EET. Future research is  
4 expected to broaden the spectrum of introduced  
5 nanomaterials to better interpret, interrogate, and engineer  
6 these EET processes. These endeavours are opening doors for  
7 ample possibilities by bridging the gap between biological and  
8 artificial electronic systems, thus eventually transforming the  
9 way we communicate with biological systems. 51  
60  
61 18  
62  
63 19  
64  
65  
66  
67 20  
68  
69 21  
70  
71 22  
72  
73 23  
74  
75 24  
76  
77  
78 25  
79  
80 26  
81  
82 27  
83  
84 28  
85  
86  
87 29  
88  
89 30  
90  
91 31  
92  
93  
94 32  
95  
96 33  
97  
98 34  
99  
100 35  
101 36  
102 37  
103  
104  
105 38  
106  
107
- 10 **Conflicts of interest**
- 11 There are no conflicts to declare
- 12 **Acknowledgements**
- 13 The authors acknowledge the support from National Science  
14 Foundation (NSF DMR-1652095), NSERC Postdoctoral  
15 Fellowships Program (PDF-487877-2016) and Tufts Summer  
16 Scholars Program.
- 17 **Notes and references**
- 18 1 H. B. Gray and J. R. Winkler, *Annu. Rev. Biochem.*, 1996, **65**,  
19 537–561.
- 20 2 A. Kumar, L. H.-H. Hsu, P. Kavanagh, F. Barrière, P. N. L.  
21 Lens, L. Lapinsoinière, J. H. Lienhard V, U. Schröder, X.  
22 Jiang and D. Leech, *Nat. Rev. Chem.*, 2017, **1**, 24.
- 23 3 B. E. Logan, B. Hamelers, R. Rozendal, U. Schröder, J. Keller,  
24 S. Freguia, P. Aelterman, W. Verstraete and K. Rabaey,  
25 *Environ. Sci. Technol.*, 2006, **40**, 5181–5192.
- 26 4 J. R. Kim, Y. E. Song, G. Munussami, C. Kim and B. H. Jeon,  
27 *Geosystem Eng.*, 2015, **18**, 173–180.
- 28 5 G. Biological and D. R. Lovley, *MBio*, 2017, **8**, e00695-17.
- 29 6 M. A. Lebedev and M. A. L. Nicolelis, *Trends Neurosci.*,  
30 2006, **29**, 536–546.
- 31 7 L. F. Nicolas-Alonso and J. Gomez-Gil, *Sensors*, 2012, **12**,  
32 1211–1279.
- 33 8 F. J. H. Hol and C. Dekker, *Science*, 2014, **346**, 1251821–  
34 1251821.
- 35 9 M. E. Hernandez, A. Kappler and D. K. Newman, *Appl.*  
36 *Environ. Microbiol.*, 2004, **70**, 921–928.
- 37 10 E. Marsili, D. B. Baron, I. D. Shikhare, D. Coursolle, J. a  
38 Gralnick and D. R. Bond, *Proc. Natl. Acad. Sci. U. S. A.*,  
39 2008, **105**, 3968–3973.
- 40 11 D. K. Newman and R. Kolter, *Nature*, 2000, **405**, 94–7.
- 41 12 L. Shi, T. C. Squier, J. M. Zachara and J. K. Fredrickson, *Mo*  
42 *Microbiol.*, 2007, **65**, 12–20.
- 43 13 L. Shi, H. Dong, G. Reguera, H. Beyenal, A. Lu, J. Liu, H.-C.  
44 Yu and J. K. Fredrickson, *Nat. Rev. Microbiol.*, 2016, **14**,  
45 651–662.
- 46 14 H. Richter, K. P. Nevin, H. Jia, D. A. Lowy, D. R. Lovley and  
47 M. Tender, *Energy Environ. Sci.*, 2009, **2**, 506.
- 48 15 Y. A. Gorby, S. Yanina, J. S. McLean, K. M. Rosso, D. Moyer,  
49 A. Dohnalkova, T. J. Beveridge, I. S. Chang, B. H. Kim, K. S.  
50 Kim, D. E. Culley, S. B. Reed, M. F. Romine, D. A. Saffarini,  
A. Hill, L. Shi, D. A. Elias, D. W. Kennedy, G. Pinchuk, K.  
Watanabe, S. Ishii, B. Logan, K. H. Nealson and J. K.  
Fredrickson, *Proc. Natl. Acad. Sci. U. S. A.*, 2006, **103**,  
11358–11363.
- S. Pirbadian, S. E. Barchinger, K. M. Leung, H. S. Byun, Y.  
Jangir, R. A. Bouhenni, S. B. Reed, M. F. Romine, D. A.  
Saffarini, L. Shi, Y. A. Gorby, J. H. Golbeck and M. Y. El-  
Naggar, *Proc. Natl. Acad. Sci. U. S. A.*, 2014, **111**, 12883–8.  
G. Reguera, K. D. McCarthy, T. Mehta, J. S. Nicoll, M. T.  
Tuominen and D. R. Lovley, *Nature*, 2005, **435**, 1098–1101.  
N. S. Malvankar and D. R. Lovley, *ChemSusChem*, 2012, **5**,  
1039–1046.
- N. S. Malvankar, M. Vargas, K. P. Nevin, A. E. Franks, C.  
Leang, B.-C. Kim, K. Inoue, T. Mester, S. F. Covalla, J. P.  
Johnson, V. M. Rotello, M. T. Tuominen and D. R. Lovley,  
*Nat. Nanotechnol.*, 2011, **6**, 573–579.
- S. M. Strycharz-Glaven and L. M. Tender, *Energy Environ.*  
*Sci.*, 2012, **5**, 6250–6255.
- N. S. Malvankar, M. T. Tuominen and D. R. Lovley, *Energy*  
*Environ. Sci.*, 2012, **5**, 6247–49.
- S. M. Strycharz-Glaven, R. M. Snider, A. Guiseppe-Elie and L.  
M. Tender, *Energy Environ. Sci.*, 2011, **4**, 4366.
- D. Coursolle, D. B. Baron, D. R. Bond and J. A. Gralnick, *J.*  
*Bacteriol.*, 2010, **192**, 467–474.
- K. P. Nevin, B. C. Kim, R. H. Glaven, J. P. Johnson, T. L.  
Woodward, B. A. Methé, R. J. Didonato, S. F. Covalla, A. E.  
Franks, A. Liu and D. R. Lovley, *PLoS One*, 2009, **4**, e5628.
- Y. Yang, M. Xu, J. Guo and G. Sun, *Process Biochem.*, 2012,  
**47**, 1707–1714.
- M. Breuer, K. M. Rosso, J. Blumberger and J. N. Butt, *J. R.*  
*Soc. Interface*, 2015, **12**, 20141117.
- D. R. Bond, S. M. Strycharz-Glaven, L. M. Tender and C. I.  
Torres, *ChemSusChem*, 2012, **5**, 1099–1105.
- A. A. Carmona-Martinez, F. Harnisch, L. A. Fitzgerald, J. C.  
Biffinger, B. R. Ringeisen and U. Schröder,  
*Bioelectrochemistry*, 2011, **81**, 74–80.
- Z. He and F. Mansfeld, *Energy Environ. Sci.*, 2009, **2**, 215–  
219.
- B. E. Logan, *Microbial Fuel Cells*, John Wiley & Sons, Inc.,  
1st edn., 2008.
- D. Das, *Microbial Fuel Cell-A Bioelectrochemical System*  
*that Converts Waste to Watts*, Springer International  
Publishing, 1st edn., 2018.
- M. Grattieri, K. Hasan and S. D. Minteer,  
*ChemElectroChem*, 2017, **4**, 834–842.
- H. Wang and Z. J. Ren, *Biotechnol. Adv.*, 2013, **31**, 1796–  
1807.
- A. P. Borole, G. Reguera, B. Ringeisen, Z.-W. Wang, Y. Feng  
and B. H. Kim, *Energy Environ. Sci.*, 2011, **4**, 4813.
- S. Choi, *Biosens. Bioelectron.*, 2015, **69**, 8–25.
- D. R. Lovley, *Curr. Opin. Electrochem.*, 2017, **4**, 190–198.
- G. Reguera, K. P. Nevin, J. S. Nicoll, S. F. Covalla, T. L.  
Woodard and D. R. Lovley, *Appl. Environ. Microbiol.*, 2006,  
**72**, 7345–7348.
- M. Y. El-Naggar, G. Wanger, K. M. Leung, T. D. Yuzvinsky, G.  
Southam, J. Yang, W. M. Lau, K. H. Nealson and Y. A. Gorby,  
*Proc. Natl. Acad. Sci.*, 2010, **107**, 18127–18131.

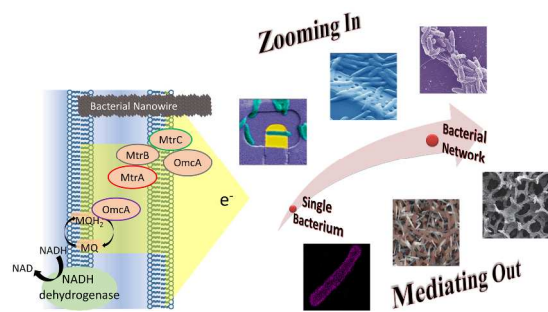
- 1 39 R. Y. Adhikari, N. S. Malvankar, M. T. Tuominen and D. R. 58 64  
 2 Lovley, *RSC Adv.*, 2016, **6**, 8354–8357. 59  
 3 40 B. F. Brehm-Stecher and E. A. Johnson, *Microbiol. Mol. Biol. Rev.*, 2004, **68**, 538–559. 60 65  
 4 41 S. V Avery, *Nat. Rev. Microbiol.*, 2006, **4**, 577. 62 66  
 5 42 X. Jiang, J. Hu, E. R. Petersen, L. a Fitzgerald, C. S. Jackan, 63 67  
 6 M. Lieber, B. R. Ringeisen, C. M. Lieber and J. C. Biffinger, 64  
 7 *Nat. Commun.*, 2013, **4**, 2751. 65  
 8 43 H. Liu, G. J. Newton, R. Nakamura, K. Hashimoto and S. 66 68  
 9 Nakanishi, *Angew. Chemie*, 2010, **122**, 6746–6749. 67  
 10 44 X. Xie, C. Criddle and Y. Cui, *Energy Environ. Sci.*, 2015, **8**, 68 69  
 11 3418–3441. 69  
 12 45 X. Jiang, J. Hu, L. A. Fitzgerald, J. C. Biffinger, P. Xie, B. R. 70 70  
 13 Ringeisen and C. M. Lieber, *Proc. Natl. Acad. Sci.*, 2010, 71  
 14 **107**, 16806–16810. 72 71  
 15 46 R. M. Snider, S. M. Strycharz-Glaven, S. D. Tsoi, J. S. 73  
 16 Erickson and L. M. Tender, *Proc. Natl. Acad. Sci.*, 2012, **109** 72  
 17 15467–15472. 75  
 18 47 M. Ding, H. Y. Shiu, S. L. Li, C. K. Lee, G. Wang, H. Wu, N. 76 73  
 19 Weiss, T. D. Young, P. S. Weiss, G. C. L. Wong, K. H. 77  
 20 Nealon, Y. Huang and X. Duan, *ACS Nano*, 2016, **10**, 9919 78 74  
 21 9926. 79  
 22 48 P. S. Bonanni, D. F. Bradley, G. D. Schrott and J. P. 80 75  
 23 Busalmen, *ChemSusChem*, 2013, **6**, 711–720. 81  
 24 49 E. Katz and I. Willner, *Angew. Chemie - Int. Ed.*, 2004, **43**, 82  
 25 6042–6108. 83 76  
 26 50 Y. Xiao, F. Patolsky, E. Katz, J. F. Hainfeld and I. Willner, 84  
 27 *Science*, 2003, **299**, 1877–1881. 85 77  
 28 51 F. Patolsky, Y. Weizmann and I. Willner, *Angew. Chemie - 86  
 29 Int. Ed.*, 2004, **43**, 2113–2117. 87 78  
 30 52 J. J. Gooding, R. Wibowo, J. Liu, W. Yang, D. Losic, S. 88  
 31 Orbons, F. J. Mearns, J. G. Shapter and D. B. Hibbert, *J. Am. 89 79  
 32 Chem. Soc.*, 2003, **125**, 9006–9007. 90  
 33 53 V. Pardo-Yissar, E. Katz, J. Wasserman and I. Willner, *J. Am. 91 80  
 34 Chem. Soc.*, 2003, **125**, 622–623. 92  
 35 54 X. Xie, L. Hu, M. Pasta, G. F. Wells, D. Kong, C. S. Criddle 93  
 36 and Y. Cui, *Nano Lett.*, 2011, **11**, 291–296. 94 81  
 37 55 X. W. Liu, J. J. Chen, Y. X. Huang, X. F. Sun, G. P. Sheng, D. 95  
 38 Li, L. Xiong, Y. Y. Zhang, F. Zhao and H. Q. Yu, *Sci. Rep.*, 96  
 39 2014, **4**, 1–7. 97 82  
 40 56 G. C. Zhao, Z. Z. Yin, L. Zhang and X. W. Wei, *Electrochem 98  
 41 commun.*, 2005, **7**, 256–260. 99 83  
 42 57 X. Xie, M. Ye, L. Hu, N. Liu, J. R. McDonough, W. Chen, H. 100  
 43 Alshareef, C. S. Criddle and Y. Cui, *Energy Environ. Sci.*, 101  
 44 2012, **5**, 5265–5270. 102 84  
 45 58 V. Flexer, J. Chen, B. C. Donose, P. Sherrell, G. G. Wallace 103  
 46 and J. Keller, *Energy Environ. Sci.*, 2013, **6**, 1291. 104 85  
 47 59 H. Yuan and Z. He, *Nanoscale*, 2015, **7**, 7022–7029. 105  
 48 60 C. e. Zhao, J. Wu, Y. Ding, V. B. Wang, Y. Zhang, S. 106 86  
 49 Kjelleberg, J. S. C. Loo, B. Cao and Q. Zhang, 107  
 50 *ChemElectroChem*, 2015, **2**, 654–658. 108 87  
 51 61 C. Ding, H. Liu, Y. Zhu, M. Wan and L. Jiang, *Energy Environ. 109  
 52 Sci.*, 2012, **5**, 8517. 110 88  
 53 62 C. Ding, H. Liu, M. Lv, T. Zhao, Y. Zhu and L. Jiang, 111  
 54 *Nanoscale*, 2014, **6**, 7866. 112 89  
 55 63 C. E. Zhao, J. Wu, S. Kjelleberg, J. S. C. Loo and Q. Zhang, 113  
 56 *Small*, 2015, **11**, 3440–3443. 114  
 57 F. A. Z. a. Alatraktchi, Y. Zhang and I. Angelidaki, *Appl. Energy*, 2014, **116**, 216–222.  
 Y. Fan, S. Xu, R. Schaller, J. Jiao, F. Chaplen and H. Liu, *Biosens. Bioelectron.*, 2011, **26**, 1908–1912.  
 X. Jia, Z. He, X. Zhang and X. Tian, *Synth. Met.*, 2016, **215**, 170–175.  
 X.-B. Gong, S.-J. You, Y. Yuan, J.-N. Zhang, K. Sun and N.-Q. Ren, *ChemElectroChem*, 2015, **2**, 1307–1313.  
 Y. Qiao, X. S. Wu and C. M. Li, *J. Power Sources*, 2014, **266**, 226–231.  
 R. Bian, Y. Jiang, Y. Wang, J. Sun, J. Hu, L. Jiang and H. Liu, *Adv. Funct. Mater.* 2018, **28**, 1707408.  
 J. Ji, Y. Jia, W. Wu, L. Bai, L. Ge and Z. Gu, *Colloids Surfaces A Physicochem. Eng. Asp.*, 2011, **390**, 56–61.  
 X. Peng, H. Yu, X. Wang, N. Gao, L. Geng and L. Ai, *J. Power Sources*, 2013, **223**, 94–99.  
 X. Peng, H. Yu, X. Wang, Q. Zhou, S. Zhang, L. Geng, J. Sun and Z. Cai, *Bioresour. Technol.*, 2012, **121**, 450–453.  
 F. Qian, H. Wang, Y. Ling, G. Wang, M. P. Thelen and Y. Li, *Nano Lett.*, 2014, **14**, 3688–3693.  
 H. Nie, T. Zhang, M. Cui, H. Lu, D. R. Lovley and T. P. Russell, *Phys. Chem. Chem. Phys.*, 2013, **15**, 14290–14294.  
 T. Zhang, H. Nie, T. S. Bain, H. Lu, M. Cui, O. L. Snoeyenbos-West, A. E. Franks, K. P. Nevin, T. P. Russell and D. R. Lovley, *Energy Environ. Sci.*, 2013, **6**, 217–224.  
 P. Zhang, J. Liu, Y. Qu, J. Zhang, Y. Zhong and Y. Feng, *J. Power Sources*, 2017, **361**, 318–325.  
 B. H. Kim, H. J. Kim, M. S. Hyun and D. H. Park, *J. Microbiol. Biotechnol.*, 1999, **9**, 127–131.  
 R. Nakamura, F. Kai, A. Okamoto, G. J. Newton and K. Hashimoto, *Angew. Chemie - Int. Ed.*, 2009, **48**, 508–511.  
 T. M. Flynn, E. J. O. Loughlin, B. Mishra, T. J. Dichristina and K. M. Kemner, *Science*, 2014, **344**, 1039–1043.  
 R. Nakamura, A. Okamoto, N. Tajima, G. J. Newton, F. Kai, T. Takashima and K. Hashimoto, *ChemBioChem*, 2010, **11**, 643–645.  
 X. Jiang, J. Hu, A. M. Lieber, C. S. Jackan, J. C. Biffinger, L. A. Fitzgerald, B. R. Ringeisen and C. M. Lieber, *Nano Lett.*, 2014, **14**, 6737–6742.  
 R. Wu, L. Cui, L. Chen, C. Wang, C. Cao, G. Sheng, H. Yu and F. Zhao, *Sci. Rep.*, 2013, **3**, 1–7.  
 X. Wu, F. Zhao, N. Rahunen, J. R. Varcoe, C. Avignone-Rossa, A. E. Thumser and R. C. T. Slade, *Angew. Chemie - Int. Ed.*, 2011, **50**, 427–430.  
 Y. Yuan, S. Zhou, B. Zhao, L. Zhuang and Y. Wang, *Bioresour. Technol.*, 2012, **116**, 453–458.  
 S. Kato, R. Nakamura, F. Kai, K. Watanabe and K. Hashimoto, *Environ. Microbiol.*, 2010, **12**, 3114–3123.  
 K. K. Sakimoto, C. Liu, J. Lim and P. Yang, *Nano Lett.*, 2014, **14**, 5471–5476.  
 L. H. H. Hsu, D. Pu, Y. Zhang and X. Jiang, *Nano Lett.*  
**DOI: 10.1021/acs.nanolett.8b01908**  
 S. Zhou, J. Tang, Y. Yuan, G. Yang and B. Xing, *Environ. Sci. Technol. Lett.*, **DOI:10.1021/acs.estlett.8b00275**.  
 M. A. Maurer-Jones, I. L. Gunsolus, B. M. Meyer, C. J. Christenson and C. L. Haynes, *Anal. Chem.*, 2013, **85**, 5810–5818.

## ARTICLE

## Journal Name

- 1 90 A. Kunzmann, B. Andersson, T. Thurnherr, H. Krug, A.  
2 Scheynius and B. Fadeel, *Biochim. Biophys. Acta - Gen.*  
3 *Subj.*, 2011, **1810**, 361–373.  
4 91 X. Xie, G. Yu, N. Liu, Z. Bao, C. S. Criddle and Y. Cui, *Energy*  
5 *Environ. Sci.*, 2012, **5**, 6862–6866  
6  
7

## Table of Contents Entry



Probing and facilitating microbial extracellular electron transfer through nanotechnology enabled platforms are transforming bioenergetic, bioelectronic, and other related research areas.